ADVANCED OPTICAL MATERIALS
www.advopticalmat.de

Aperiodic Metal-Dielectric Multilayers as Highly Efficient Sunlight Reflectors

*Alberto Jiménez-Solano, Miguel Anaya, Mauricio E. Calvo, Mercedes Alcon-Camas, Carlos Alcañiz, Elena Guillén, Noelia Martínez, Manuel Gallas, Thomas Preussner, Ramón Escobar-Galindo, and Hernán Míguez**

The optimum reflection of the solar spectrum at well-defined incident directions as well as its durability in time are, both, fundamental requirements of the optics of thermosolar and photovoltaic energy conversion systems. The stringent high performance needed for these applications implies that, almost exclusively, second face mirrors based on silver are employed for this purpose. Herein, the possibility to develop solar mirrors using other metals, such as copper and aluminum, is theoretically and experimentally analyzed. It is found that reflectors based on these inexpensive metals are capable of reflecting the full solar spectrum with efficiencies comparable to that of silver-based reflectors. The designs herein proposed are based on aperiodic metal-dielectric multilayers whose optimized configuration is chosen employing a code based on a genetic algorithm that allows selecting the best one among 10^8 tested reflectors. The use of metals with wider spectral absorption bands is compensated by the use of multilayered designs in which metal absorption is almost suppressed, as the analysis of the electric field intensity distribution demonstrates. The feasibility of the proposed mirrors is demonstrated by their actual fabrication by large area deposition techniques amenable for mass production.

For numerous applications in the field of solar energy, management of sunlight is achieved by means of broadband highly reflecting mirrors. Such is the case, for instance, in concentrated solar power (CSP) plants,[1] photovoltaic[2] and thermophotovoltaic systems,[3] and even in sophisticated radiative cooling units.[4] In the case of CSP, ultrabroadband (300 nm < λ < 2500 nm) reflection is actually required, since energy conversion efficiency depends strongly on the ability to concentrate the full solar spectrum onto the fluid carrying absorber tube at the solar receiver. Due to their high reflecting properties in most of the solar irradiance band, silver mirrors have been so far the preferred choice for this purpose.[5] Silver coatings on glass are usually realized by either sputtering or chemical bath deposition, both processes are suitable for mass production and hence compatible with the large surface coverage required for the above mentioned applications. Apart from high reflectivity, solar mirrors require to be durable for long periods of time and resist the typically harsh environmental conditions under which they operate in the open field, such as wind, dust, moisture, or rain. This motivates that most commonly found solar mirrors present a second face configuration, i.e., the reflecting coating is deposited on extra clear glass and then backward protected with a layer of varnish. A scheme of the system can be found in Figure S1 of the Supporting Information. By protecting the silver coating in this way, its exposure to the environment, and hence its degradation, i.e., tarnishing, is prevented.[6,7] With the second face configuration and assuming extra clear glass, the maximum reflected power achievable amounts to ≈95% of the total solar luminous power received by the mirror.[8] Sources of loss are the poor UV and blue reflecting properties of the silver coating, highly absorbing in that spectral range, and the residual absorption of the sheltering glass, unavoidable even in the clearest ones commercially available.[9] Although silver mirrors have demonstrated to perform well as solar reflectors, it would be desirable to employ other less expensive metals for this purpose, such as aluminum or copper, whose prices are around two orders of magnitude lower than that of silver. Unfortunately, both have been discarded until now, due to their poor reflectance for wavelengths below 1000 nm. Although it is well known that a metal reflector can be enhanced by coating it with a layered dielectric structure,[9,10] the question of whether or not optical

A. Jiménez-Solano, M. Anaya, Dr. M. E. Calvo, Prof. H. Míguez
Multifunctional Optical Materials Group
Institute of Materials Science of Seville
Spanish National Research Council
University of Seville
Calle Américo Vespucio 49, 41092 Seville, Spain
E-mail: h.miguez@csic.es

Dr. M. Alcón-Camas, C. Alcañiz, Dr. E. Guillén, N. Martínez, Dr. M. Gallas, Dr. R. Escobar-Galindo
Abengoa Research S. L.
Campus Palmas Altas
Calle Energía Solar 1, 41014 Seville, Spain

T. Preussner
Division Flat and Flexible Products, Fraunhofer Institute for Organic Electronics
Electron Beam and Plasma Technology FEP
Winterberstrasse 28, 01277 Dresden, Germany

DOI: 10.1002/adom.201600833

interference effects occurring within realistic metal-dielectric mirrors can give rise to full sunlight reflection values similar to or even higher than silver reflectors remains unanswered. The solution to this problem depends both on the existence of a design capable of reaching those high reflectance values and on the actual feasibility of the proposed design.

Herein, we show that metal-dielectric coatings based on alternative inexpensive metals, such as copper or aluminum, can be devised and realized to achieve highly efficient solar mirrors that can outperform silver based ones.

The champion structures are in all cases made of a metal thin film coupled to an aperiodic dielectric multilayer, whose structure has been optimized to maximize full solar spectrum reflectance and minimize the absorption occurring in the metal. The multilayer is first deposited on an extra clear glass and subsequently coated by a metal film. With this approach, mirrors capable of reflecting as much as 93% of the sunlight power they receive are fabricated. Central to the concept herein proposed is the optimization procedure employed, based on the analysis of a substantial number (10^8) of potentially highly reflecting solar mirrors through a code based on a genetic algorithm, which renders stable solutions for the fittest mirrors after $\approx 10^6$ iterations. Tolerance of the optimized designs to different degrees of deviation with respect to the ideal building parameters is also analyzed, confirming the robustness and viability of the approach herein proposed. The actual realization of some of the paradigmatic designs described yields what can be considered, to the best of our knowledge, the highest silver-free reflecting solar mirrors reported up to date. Initial indoors accelerated degradation tests carried out in weather and dust chamber indicates that the so built mirrors are promising candidates for applications in CSP and photovoltaic technology.

A sound and unambiguous figure of merit to evaluate the performance of a solar mirror is the solar spectrum weighted integrated reflectance (SSWIR), defined as

$$\mathrm{SSWIR} = \frac{\int_{300}^{2500} R(\lambda)\,\mathrm{AM1.5}(\lambda)\,\mathrm{d}\lambda}{\int_{300}^{2500} \mathrm{AM1.5}(\lambda)\,\mathrm{d}\lambda} \quad (1)$$

where AM1.5(λ) is the solar direct irradiance (W m^{-2} nm^{-1}) spectrum on the earth surface usually employed as standard and $R(\lambda)$ is the reflectance of the mirror. Wavelength integration range is taken between 300 and 2500 nm, outside which the percentage of solar energy reaching the ground can be neglected. The result of Equation (1) was compared for a vast number (10^8) of mirrors employing a sequential optimization process based on the use of a genetic algorithm. Please note that, although optical interference is a wavelength dependent phenomenon, our figure of merit is not. The interference effects occurring in the multilayer of choice after each optimization round give to a maximized integrated reflectance given by Equation (1). Aluminum and copper were chosen as metals, while the dielectric materials of choice were dense silicon and titanium dioxides, since it is well known that SiO_2 and TiO_2 can be combined in multilayers to achieve highly reflecting stacks and can be prepared employing a wide variety of techniques.[11–13] The spectral dependence of the optical constants of all materials considered was provided by Fraunhofer FEP (manufacturer) and can be found in Figure S2 (Supporting Information). Calculations start by considering a single metal oxide layer on extra clear glass and a metal coating. Subsequent metal oxide layers are gradually added following a procedure that is described in full detail in Figure S3 (Supporting Information). In brief, the first set of individuals of a specific generation of solar mirrors containing N layers is attained by random combination of the characteristics of those belonging to the previous generation (and hence having $N-1$ layers) that had displayed better performance, i.e., a higher figure of merit. Subsequent crossing yields a new set of fittest individuals, which are in turn hybridized to create the $(N+1)$ layer generation. The optimization stops when a stable value of SSWIR is attained, i.e., no improvement is observed after adding a new layer to the system. To minimize dependence of the optimized design on the initial conditions and its specific stochastic evolution, the above-mentioned process is repeated 2^{10} times for 2^9 initial populations. With this amount of threads, a constant standard deviation over the whole set is ensured (Figure S4, Supporting Information).

The evolution of the optimized SSWIR, calculated for a series of metal-dielectric multilayers as a function of the number of layers in the stack, is plotted in **Figure 1**a, and they are compared with reflectance of the standard silver mirror. In this case, the mirrors are devised to show maximum integrated specular reflection at 20° incident angle, although they can be designed to perform optimally for an arbitrary direction of incident light. Interestingly, mirrors made out of copper, although of very poor performance when only the metal reflection is considered (SSWIR = 78.5%), reach SSWIR values higher than those attained with silver mirror (dashed line in Figure 1a) after adding a multilayer (95.0% vs 92.6%). In addition, they perform better than optimized aluminum-based mirrors (94.2%), whose broad absorption band makes more difficult to find a structure that can compensate for those optical losses. In general, SSWIR saturates when $N > 20$, although the specific value depends on the particular mirror under consideration. Please notice that, since the reflectance of the system depends on the constructive interference between beams being partially reflected at each interface present in the stack, the values of all layers are constantly being revised. So, although the number of layers grows continuously, the total thickness might not, and could even decrease. This effect is shown in Figure S5 (Supporting Information). In Figure 1b, the actual sequence of layers for the optimized copper- (top panel) and aluminum-based (bottom panel) solar mirrors is explicitly shown, layers composition and layers thickness are described in Table S8 (Supporting Information). It should also be remarked that a mirror with similar performance could be built by using exclusively dielectric multilayers. However, this would imply the use of hundreds of layers even with high refractive index contrast layers,[14] and not just a few tens like in the designs herein reported. The calculated reflectance spectrum at the incidence angle of choice, of the best solar mirrors attained for each one of the metal-dielectric combinations are plotted in Figure 1c along with the AM1.5 solar irradiance spectrum. The comparison between them reveals that the optimization process gives rise to structures that present reflectance minima located at the same spectral positions at which the atmosphere strongly

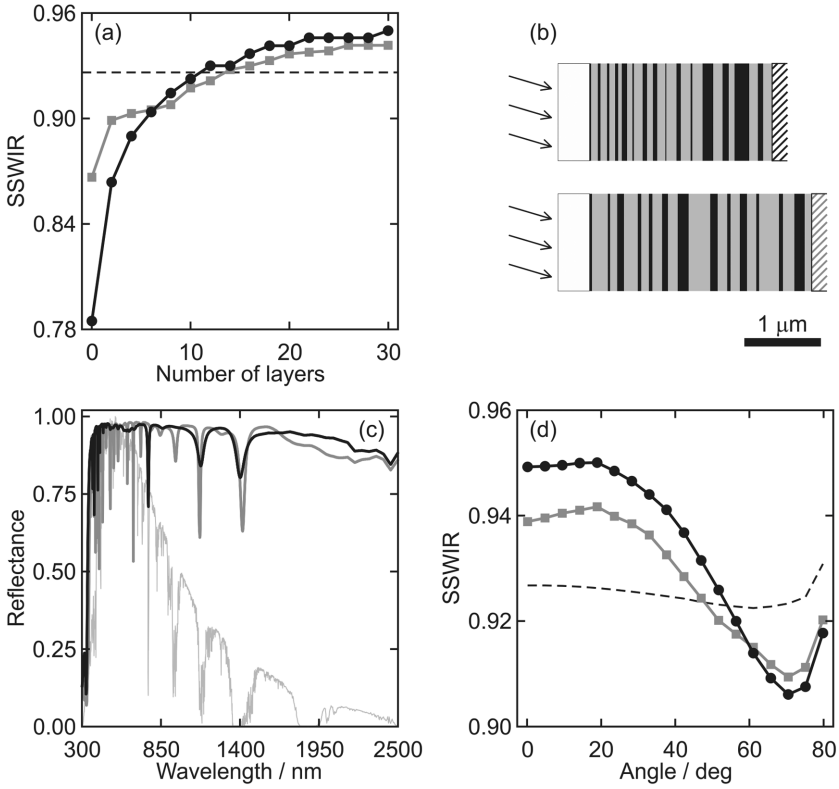

Figure 1. a) Evolution of the SSWIR of copper- (black circles) and aluminum-based (gray squares) mirrors as a function of the number of layers, dashed line shows the SSWIR of a standard silver mirror. b) Multilayer layout for the best copper- (top panel) and aluminum-based (bottom panel) mirrors. TiO_2, SiO_2, and glass are represented by colored black, gray, and white rectangles, respectively. Metal films are represented by striped rectangles. c) Calculated reflectance spectra for the best copper- (black) and aluminum-based (gray) mirrors along with the AM1.5 solar irradiance spectrum (light gray). d) Angular response for the best copper- (black circles) and aluminum-based (gray squares) solar mirrors together with the angular response of a standard silver mirror (dashed line).

absorbs the incoming radiation. The wavelength at which each one of these dips occurs blue-shifts with increasing angle of incidence. In principle, this could affect the performance at angles different to those for which the solar mirror reflectance was optimized. Figure 1d shows the SSWIR as a function of the incident angle for the best copper- and aluminum-based solar mirrors together with the angular response of a standard silver mirror.

A remarkable feature of the design herein presented is the minimization of the optical losses caused by absorption within the metal layer. This is achieved by diminishing the electromagnetic field intensity within the metal at those wavelengths for which it presents higher losses. In practical terms, the high broadband reflection is the result of the combined effect of the metal and the multilayer. The design of the multilayer is such that allows NIR wavelengths to reach the metal, as it presents no losses and a high reflectivity in that range. In the visible and UV regions, where the metal presents a higher extinction coefficient, the dielectric multilayer reflects more effectively. This can be explicitly seen in **Figure 2**a, in which we plot the absorptance of a self-standing copper layer (gray solid line) and compare it to that of the optimized solar mirror herein reported (black solid line). The AM1.5 solar irradiance spectrum is drawn for the sake of comparison. The power absorbed by metal layer is evaluated using the expression

$$P_{\mathrm{abs}}(\omega) = \omega\varepsilon_0 \int |E(x,\omega)|^2 \, n(\omega)k(\omega)\,\mathrm{d}x \qquad (2)$$

where ω is the angular frequency, ε_0 is the dielectric constant of vacuum, $E(x, \omega)$ the electric field, x is the relative position within the layer, and $n(\omega)$ and $k(\omega)$ are the spectrally dependent real and imaginary parts of the refractive index of the metal. The corresponding spatial distributions of the normalized electric field intensity along the self-standing and the multilayer coated metal films are plotted in Figure 2b,c, respectively. In all cases, light impinges from below and first encounters the metal at the position labeled as zero. It can be readily seen that metal absorptance is largely diminished in the UV and visible range of the spectrum for the case of the metal film coupled to the dielectric multilayer in the solar mirror. Interestingly, it is reinforced at some specific near infrared frequencies which, however, do not contribute to the losses as they coincide with spectral ranges at which the solar irradiance on the Earth surface vanishes. This is the reason why the solar spectrum weighted absorptance is practically null at those specific longer wavelengths, regardless the configuration in which the metal film is used, as it can be seen in the series of Figure 2d,f. How the mirror design prevents the ultraviolet and visible electromagnetic fields to reach the metal can be inferred from the scheme of the optimized copper-based mirror drawn in the upper panel of Figure 1b. In it, the thinnest layers of any composition tend to be further away from it, hence giving rise first to efficient short wavelength reflection and letting the rest of sunlight frequencies propagate through the multilayer. Dielectric layers tend to be gradually thicker as the metal layer is approached, favoring near infrared reflection from deeper parts of the mirror.

Figure 3 shows the angular dependence of mirrors herein optimized as a function of the number of layers for copper- and aluminum-based solar mirrors optimized at 20°. However, it is also possible to design solar mirrors that maximize their response for a wide range of angles simultaneously and hence display a robust angular response. In Figure S6 (Supporting Information), we plot the angular response of one mirror the performance of which was maximized in the range between 0° and 40° and compare it to the one optimized considering only the figure of merit at 20°. As expected, the averaged angular response in the whole range is higher for the former.

In order to evaluate the viability of the proposed designs, we had metal-dielectric multilayer mirrors manufactured by

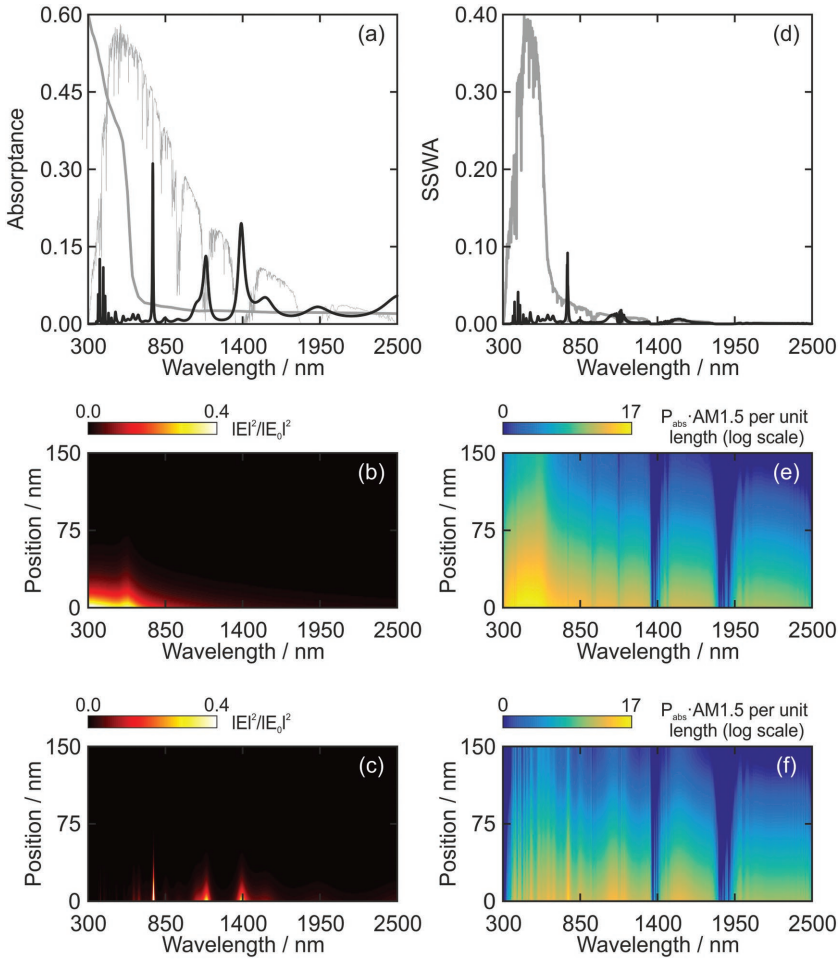

Figure 2. a) Absorptance of a self-standing cooper film (gray line) and for the same film integrated in a 30 layer mirror (black line), along with the AM1.5 solar irradiance spectrum (light gray line). b,c) Spatial distribution of the normalized electric field intensity within a self-standing copper film and for the same film integrated in a 30 layer mirror mirrors. d) Solar spectrum weighted absorptance of the same layers shown in panel (a), a equivalent color code being followed. e,f) Spatial distribution of the solar spectrum weighted power absorbed (in log scale) per unit length of the same systems showed in panels (b) and (c), respectively.

pulsed magnetron sputtering at the Fraunhofer Institute for Organic Electronics, Electron Beam and Plasma Technology FEP, whose physical vapor deposition facilities can be subcontracted to realize a predesigned structure. In this laboratory, large substrates areas (up to 60 cm × 120 cm) can be uniformly coated and the thickness of each film in the stack can be determined with a precision of 1%–3% of the nominal thickness. Full details can be found in the Experimental Section. **Figure 4** displays images of manufactured copper-based mirrors. A 22 layer copper-dielectric multilayer was the preferred choice as a greater performance as solar reflectors are expected from the calculations. Figure 4b shows a view of the back side, from which the colored copper layer deposited can be observed. Figure 4c shows a view of the cross section of one of these copper-based mirrors when observed under a field-emission scanning electron microscope (FESEM), in which its multilayered structure is explicitly revealed.

The reflection properties in the full solar spectrum wavelength range at variable angles were studied by using an absolute measurement unit. Reflectance curve for the manufactured copper-dielectric layered mirror is displayed in **Figure 5**a along with the corresponding theoretical predictions. From the experimental data, SSWIR is estimated to be 93.0% in good agreement with theoretical predictions (94.6%). In order to quantify the effect of the occurrence of thickness deviations with respect to the theoretical values during the manufacturing process, a tolerance analysis was carried out. To do so, we let the thickness of each layer to take arbitrary values t_i around the optimal one T_i and comprised within a range determined by a certain percentage of that value. For each one of these deviation ranges we calculate the SSWIR. Results are plotted in Figure 5b. It can be seen that the SSWIR of the mirrors are maintained above the optimized value, for deviations as large $\Delta t_i = 5\%$ with $\sigma < 6 \times 10^{-4}$. Hence, the deviance observed in the experimental reflectance from that of the optimized designs may be understood as the result of the difference between the tabulated frequency dependent refractive indexes of the materials employed and those of the actual layers finally deposited. For instance, it has been observed that thicker titania layers tend to have a higher crystallinity than thinner ones, thus influencing its optical properties. Regarding the mirror stability, in principle, copper-based mirrors should show as much durability as silver ones, as they can be devised to present the same level of front and rear protection. In order to prove so, a sample of the copper-based second face mirror was exposed to actual environmental operation conditions in the solar field for one year, no degradation in the materials or their performance being

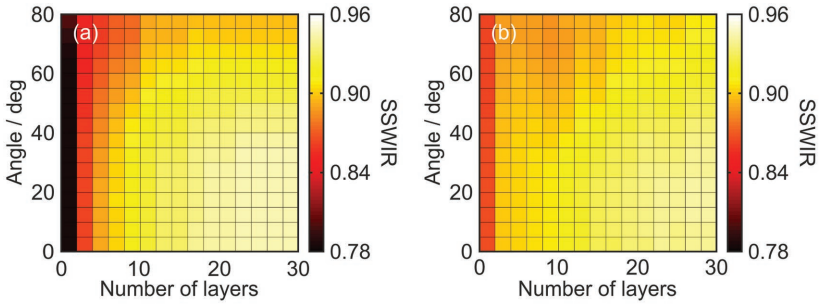

Figure 3. Angular response of the SSWIR of a) copper- and b) aluminum-based mirrors optimized at 20°.

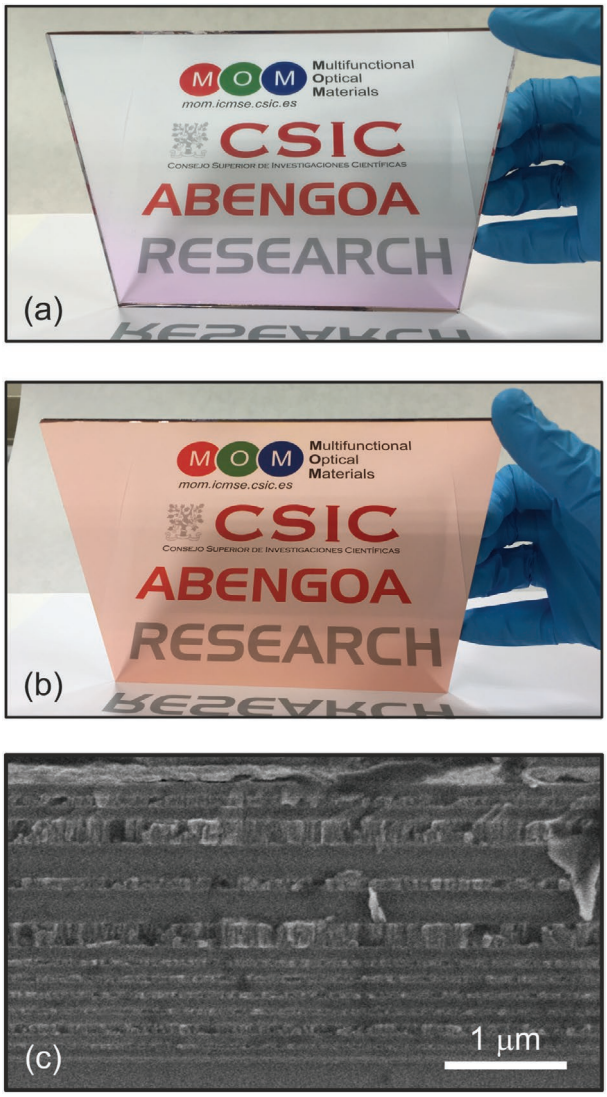

Figure 4. a,b) Images of a manufactured second face copper-based mirror taken from the front and from the rear part of the mirror. c) Representative cross section of an FESEM image extracted from a copper-based mirror. The glass substrate is the last material at the bottom of the image.

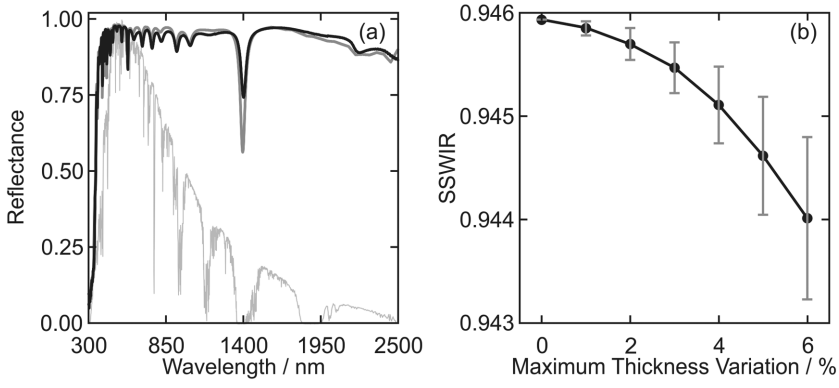

Figure 5. a) Theoretical (gray) and experimental (black) reflectance for the copper-based mirror manufactured along the AM1.5 solar spectrum (light gray). b) SSWIR as a function of maximum thickness variation. Black dots correspond to the mean value and error bars are given by the standard deviation of each set of calculation.

Table 1. Experimental deposition parameters employed to grow each type of layer present in the mirrors.

Material	Power density [W cm^{-2}]	Dynamic deposition rate [nm m min^{-1}]	Cathode type
Al, Cu	3.5	≈40	Single magnetron
SiO_2	6	≈50	Dual magnetron
TiO_2	5	≈15	Dual magnetron

detected whatsoever. Figure S7a,b (Supporting Information) shows the evolution of the SSWIR of the mirror exposed to the environment, superimposed to the recorded variations of temperature and humidity, respectively, during the same period. Figure S7c (Supporting Information) displays a picture of the mirror taken after such exposure.

In conclusion, we have demonstrated that it is possible to design and manufacture metal-dielectric multilayered solar mirrors that can outperform silver reflectors commonly employed in thermosolar and photovoltaic systems. An optimization code based on a genetic algorithm allowed us analyzing 10^8 structures and found the configuration that presented the best reflection properties among them. Copper-based mirrors were shown to display the best properties among the evaluated metals and were built and successfully tested to prove the feasibility of the proposal. These designs constitute a novel family of enhanced solar mirrors based on inexpensive metals suitable to substitute silver metals for applications in which high performance is required.

Experimental Section

Numerical Simulations: A homemade code based on a combination of the transfer matrix formalism[15] (to calculate the optical response of the sample structure) and a genetic algorithm (to search for the optimum target value, highest SSWIR) was developed.

Multilayer Deposition: The coatings were prepared by pulsed magnetron sputtering in the inline coating machine ILA750 (component length 750 mm) in dynamic mode with moved substrates. For the deposition of the metallic layers Cu and Al, single magnetron systems were used. In case of the dielectric materials SiO_2 and TiO_2, reactive pulsed sputtering with dual magnetron systems was applied. The main sputtering parameters are given in the **Table 1**. Note that the chosen set of parameters is optimized for a long-term stable and reproducible deposition of multilayer stacks.

Optical Characterization: The reflection properties in the full solar spectrum wavelength range at variable angles were studied by using a universal measurement accessory attached to a UV–vis–NIR spectrophotometer (Cary 5000).

Structural Characterization: FESEM images of cross sections of the films were taken with a Hitachi S4800 microscope operating at 2 kV.

Supporting Information

Supporting Information is available from the Wiley Online Library or from the author.

Acknowledgements

The research leading to these results was funded by Abengoa Solar New Technologies S.A. and Abengoa Research S.L. under private contracts with CSIC. Results herein presented are protected under Spanish patent P201431774.

Received: October 10, 2016
Revised: December 16, 2016
Published online: March 15, 2017

[1] M. Roeb, M. Neises, N. Monnerie, C. Sattler, R. Pitz-Paal, *Energy Environ. Sci.* **2011**, *4*, 2503.
[2] B. Curtin, R. Biswas, V. Dalal, *Appl. Phys. Lett.* **2009**, *95*, 231102.
[3] P. Bermel, M. Ghebrebrhan, W. Chan, Y. X. Yeng, M. Araghchini, R. Hamam, C. H. Marton, K. F. Jensen, M. Soljacic, J. D. Joannopoulos, S. G. Johnson, I. Celanovic, *Opt. Express* **2010**, *18*, A314.
[4] E. Rephaeli, A. Raman, S. Fan, *Nano Lett.* **2013**, *13*, 1457.
[5] F. Sutter, S. Meyen, A. Fernández-García, P. Heller, *Sol. Energy Mater. Sol. Cells* **2016**, *145*, 248.
[6] M. Brogrena, B. Karlsson, A. Roos, A. Werner, *Sol. Energy Mater. Sol. Cells* **2004**, *82*, 491.
[7] T. Sarver, A. Al-Qaraghuli, L. L. Kazmerski, *Renewable Sustainable Energy Rev.* **2013**, *22*, 698.
[8] P. Good, T. Cooper, M. Querci, N. Wiik, G. Ambrosetti, A. Steinfeld, *Sol. Energy Mater. Sol. Cells* **2016**, *144*, 509.
[9] G. P. Butel, B. M. Coughenour, H. A. Macleod, C. E. Kennedy, J. R. P. Angel, *J. Photonics Energy* **2012**, *2*, 021808.
[10] F. Sutter, S. Ziegler, M. Schmücker, P. Heller, R. Pitz-Paal, *Sol. Energy Mater. Sol. Cells* **2012**, *107*, 37.
[11] S. Colodrero, M. Ocaña, H. Míguez, *Langmuir* **2008**, *24*, 4430.
[12] K. M. Chen, A. W. Sparks, H.-C. Luan, D. R. Lim, K. Wada, L. C. Kimerling, *Appl. Phys. Lett.* **1999**, *75*, 3805.
[13] S. Jena, R. B. Tokas, P. Sarkar, J. S. Misal, S. M. Haque, K. D. Rao, S. Thakur, N. K. Sahoo, *Thin Solid Films* **2016**, *599*, 138.
[14] A. D. Ariza-Flores, L. M. Gaggero-Sager, V. Agarwal, *Appl. Phys. Lett.* **2012**, *101*, 031119.
[15] P. Yeh, *Optical Waves in Layered Media*, Wiley, New York **1988**.